Proceedings of ASME Turbo Expo 2011
GT2011
June 6-10, 2011, Vancouver, British Columbia, Canada

GT2011-46431

AN ACOUSTIC METHODOLOGY TO MEASURE HEAT RELEASE RATE FLUCTUATIONS FROM UNSTEADY LAMINAR FLAMES

J. Li[*]**, F. Richecoeur, T. Schuller**
Laboratoire EM2C, Ecole Centrale Paris and CNRS, Chtenay-Malabry 92295,France
Email: jingxuan.li@em2c.ecp.fr
Y. Huang
School of Jet Propulsion, Beijing University of Aeronautics and Astronautics, Beijing 100083, China

ABSTRACT

This paper presents first validations of an alternative method to optical diagnostics to evaluate unsteady heat release rate disturbances. The technique is based on the determination of the propagation time of ultrasonic waves crossing a reacting flow. A train of pulses is synthesized and transmitted to the space by a tweeter. This signal is captured before and after its passage through the flame. The cross-correlation of the two signals yields a narrow compressed pulse response with a main lobe corresponding to the time lag between the incident and transmitted signals. The technique is examined in two generic laminar configurations. For open flames featuring buoyancy effects, it is possible to link the rate of change of fluctuations of the sound travel time $d\Delta t'/dt$ to heat release rate disturbances $\dot{Q}'$. For pulsated confined flames, the situation is more complex and a transfer function must be defined between perturbations in the sound travel time $\Delta t'$ and heat release rate disturbances $\dot{Q}'$. Measurements are compared to predictions using different techniques. A general agreement is obtain in term of phasing and amplitudes. This study shows that the proposed technique is very sensitive to small perturbations in the heat release rate and provides the basis for further developments oriented towards more practical configurations.

NOMENCLATURE

A Section area of burner [m^2]
A_f Flame area [m^2]
B Chirp frequency bandwidth [Hz]
c Speed of sound [m s^{-1}]
c_p Specific heat capacity [J kg^{-1}]
f_i Initial frequency of chirp signal [Hz]
f_m Modulation frequency [Hz]
I Light-emission intensity measured in Volt [V]
k Coefficient between heat release rate $\dot{Q}$ and light-emission intensity I.
L Acoustic path length [m]
L_f Characteristic length of the burned gases [m]
$\dot{m}$ Mass flow rate [kg s^{-1}]
p Pressure [Pa]
$\dot{Q}$ Heat release rate [W]
R_{corr} Correlation between S_t and S_i .
S_L Flame speed [m s^{-1}]
S_i Incident chirp signal [-]
S_t Transmitted chirp signal [-]
t_r Repetition time of the chirp signal [s]
t Time [s]
T Temperature [K]
v Flow velocity [m s^{-1}]
V Gas volume [m^3]
Δt Sound propagation time [s]
τ Time duration of chirp signal [s]
γ Specific heat capacity ratio [-]
β Amplitude of the chirp signal [-]
α Proportionality coefficient.

[*]Address all correspondence to this author.

ρ Gas density [kg m^{-3}]
Ξ Coefficient between variations of propagation time dΔt/dt and light-emission intensity fluctuation I'.
ϕ Gas mixture equivalence ratio [-]
$_u$ Unburned gas
$_b$ Burned gas
$\bar{}$ Mean component
$'$ Fluctuating component

1 Introduction

Heat release rate disturbances are the sources of unsteady thermal stresses, they generate indirect combustion noise when the flow is accelerated through turbines or a convergent nozzle and may even cause destructive combustion instabilities [1]. These perturbations are difficult to measure and are generally determined using optical techniques. The chemiluminescence emission from the naturally excited radicals formed within the flame front, such as OH^*, CH^* and C_2^*, is often considered as a good marker of heat release rate [2–6]. This is generally admitted in well premixed flames if the composition is uniform. Fluctuations in the light emission intensity of these radicals is then proportional to the flame surface area and heat release rate disturbances [7]. More sophisticated techniques can be used like laser induced fluorescence (LIF) for quantitative estimates of the heat release rate (see for example [8, 9]). These methods require high power well-tuned laser beams at different wavelengths and have been tested yet only in well controlled generic configurations. There is thus a need for the development of alternative techniques to determine heat release rate perturbations when the reactants are not perfectly mixed or when optical access is limited. The objective of this paper is to present one possible alternative based on an acoustic technique. The principle of this new method is introduced and first validations in well controlled generic configurations are presented.

The technique is based on the determination of the sound travel time of ultrasonic waves in reacting flows. ultrasonic waves do not interact with the flame or the flow due to their high frequency [10]. The link between perturbations in the travel time of sound waves crossing flames with perturbations in the heat release rate is examined in Section 2. The situation is different if the flame is open or confined. The experimental methodology used to determine the travel time of sound waves and the corresponding signal post-processing are presented in Section 3. This relies on a pulse compression technology used in radars. The experimental arrangement and the two configurations explored are then presented in Section 4. The first one corresponds to a conical premixed flame stabilized on the nozzle of a laminar burner. This flame features small low frequency heat release rate perturbations due to buoyancy effects. The second one considers a laminar conical flame confined within a flame tube and submitted to harmonic modulations. Measurements and comparisons with predictions are presented in Sections 5 and 6. The validations in generic configurations are promising and help to identify the main progress for further development of the proposed technique.

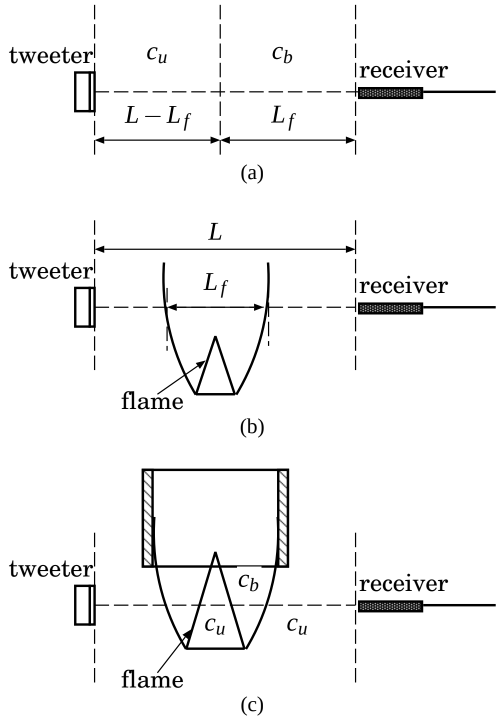

Figure 1. SCHEMATIC VIEW OF THE EXPERIMENTAL CONFIGURATION.

2 Heat release rate and sound travel time

Consider the case of a sound wave crossing a homogeneous gas at a fixed temperature and composition characterized by a speed of sound c_u over a path length L. Knowing the acoustic path length L, the propagation time Δt_0 can be deduced from the equation

$$\Delta t_0 = \frac{L}{c_u} \tag{1}$$

When the acoustic path crosses a different medium, the speed of sound in this region is modified and the propagation time is in turn also modified. This configuration is shown in Fig. 1(a) where acoustic waves emitted by a tweeter propagate through two different media. This second gas is characterized by a speed of sound c_b and extends over a length L_f along the acoustic path. The first gas now occupies a length $L-L_f$. In this configuration, Eqn. 1 is modified and the propagation time Δt over the distance L from the emitter to the receiver is now given by

$$\Delta t = \frac{L - L_f}{c_u} + \frac{L_f}{c_b} = \Delta t_0 - \frac{L_f}{c*} \quad (2)$$

where $c* = c_b c_u/(c_b - c_u)$ is an equivalent sound speed. Consider now perturbations in the distance L_f. This may for example take place in open configurations for flames stabilized on the rim of a burner due to the influence of gravity. Buoyancy effects are known to induce a low frequency oscillation of the flame plume due to a shear layer instability between the hot combustion products and the surrounding ambient air [11, 12]. This results in turn in small perturbations in the heat release rate and in fluctuations of the volume of the burned gases and the length of the acoustic path L_f. This configuration is envisaged in Fig. 1(b) where the acoustic path crosses the burned gases characterized by a speed of sound c_b which are surrounded by fresh air with a speed of sound c_u. In confined combustors, it is possible to envisage a second configuration as in Fig. 1(c) where the burned gases characterized by a speed of sound c_b are separated from the fresh reactants characterized by a speed of sound c_u. When the flame is wrinkled due for example to a self-sustained oscillation [1] or when it is submitted to flow modulations [13] this produces perturbations in the heat release rate which are accompanied by disturbances in the path length L_f. In both case, this also corresponds to fluctuations in the travel time of sound waves

$$\Delta t' = -\frac{L'_f}{c*} \quad (3)$$

In this expression only disturbances in the acoustic path length L_f are taken into account, fluctuations in the temperature and composition of the gases in the fresh and hot gases are neglected. This approximation is valid as long as relative fluctuations of $c*'/\overline{c*}$ remain small. In air combustion systems, fluctuations in the gases composition can be neglected due the large dilution with nitrogen.

It is now worth examining the link between fluctuations in the sound travel time $\Delta t'$ and perturbations in the heat release rate $\dot{Q}'$. This relation depends on the case considered. Starting with confined flames surrounded by hot gases, it is well known that perturbations in the shape of the flame produce heat release rate disturbances. This has for example been used to derive expressions for heat release rate perturbations induced by different types of flow modulations [14–18]. These relations are generally expressed in the frequency domain and take the form of flame transfer functions which depend on the frequency of the flow disturbances. For the configuration presented in Fig. 1(c), it is then natural to consider the link between heat release rate fluctuations $\dot{Q}'$ and perturbations in the acoustic path length L'_f in the frequency domain $a' = \tilde{a}\exp(-i\omega t)$:

$$\widetilde{\Delta t} = \frac{\widetilde{L_f}}{c*} = \xi(\omega)\widetilde{\dot{Q}} \quad (4)$$

In this expression the proportionality coefficient ξ is a complex number that depends on the shape of the flame, the flow operating conditions, the experimental setup and the flow disturbances frequency. It is probably possible to obtain an analytical expression of this coefficient in the frequency domain but this is beyond the scope of the present study. Measurements are however presented in Section 6 for a laminar conical flame submitted to harmonic flow modulations. Two forcing frequencies are considered and it is shown that $\widetilde{\Delta t}$ is proportional to $\widetilde{\dot{Q}}$ at each forcing frequency, the coefficient ξ being smaller at higher frequencies with a larger phase shift.

In the open flame configuration presented in Fig. 1(b) ultrasonic waves travel through the surrounding fresh air bounding the hot plume of a flame. Buoyancy effects generate low frequency periodic oscillations of the hot plume width L'_f. It is possible to link these fluctuations to the induced heat release rate perturbations. The main step of the derivation are presented here. The volume of the burned gases V_b depends on the flame surface area A_f

$$V_b = \alpha L_f A_f \quad (5)$$

where L_f is the apparent dimension of the burned gases in the line of sight of the microphones and α is a constant coefficient. For a premixed flame, a mass balance between the burner outlet and the flame front yields $v_u A = S_L A_f$, where S_L is the laminar flame speed and v_u the flow velocity at the burner outlet. It is then possible to obtain an expression of the hot plume width L_f as a function of the burned gases volume

$$L_f = \frac{S_L}{\alpha v_u A} V_b$$

In this expression, S_L only depends on the equivalence ratio, v_u is kept constant and α is time independent so that L_f can be substituted in Eqn. 3

$$\Delta t' = -\frac{S_L}{\alpha v_u A c*} V'_b \quad (6)$$

Fluctuations in the travel time of sound waves are proportional to fluctuations in the volume of burned gases V'_b. The purpose of the following paragraph is to express fluctuations of the burned gases

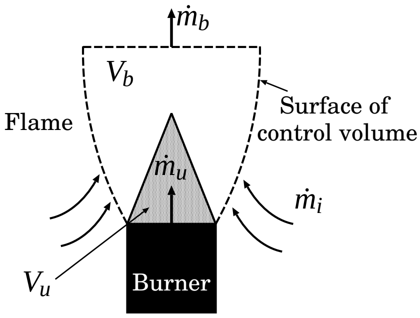

Figure 2. SCHEMATIC OF THE CONTROL VOLUME DIVIDED IN TWO PARTS BY THE FLAME: UNBURNED GASES (VOLUME V_u AND MASS FLOW $\dot{m}_u$) AND BURNED GASES (VOLUME V_b AND MASS FLOW $\dot{m}_b$).

volume as a function of heat release rate disturbances. For buoyancy driven oscillations, the flow can be considered isobaric. Using the simplified model presented in Fig. 2, a global energy balance over the control volume yields

$$\frac{\gamma p}{\gamma-1}\left(\frac{\partial V_u}{\partial t}+\frac{\partial V_b}{\partial t}\right)=\dot{m}_u c_p T_u-\dot{m}_b c_p T_b+\dot{Q} \tag{7}$$

where the lateral surface of the control volume in contact with ambient air is supposed impermeable ($\dot{m}_i = 0$) and adiabatic ($\dot{Q}_i = 0$). A first order perturbation analysis at low frequency yields

$$\frac{\gamma}{\gamma-1}p\frac{\partial V_b'}{\partial t}=\dot{Q}' \tag{8}$$

where fluctuations in the fresh reactants volume were neglected since $V_u/V_b \approx \rho_b/\rho_u = T_u/T_b \ll 1$. Combining Eqns. 6 and 8, one finally finds that heat release rate disturbances induced by buoyancy effects are proportional to the rate of change of the sound propagation time through the hot plume gases

$$\dot{Q}'=-\frac{\gamma p}{\gamma-1}\frac{\alpha v_u A c*}{S_L}\frac{\partial \Delta t'}{\partial t} \tag{9}$$

This last relation shows that it is possible to estimate heat release rate perturbations induced by flame flickering from fluctuations in the sound propagation time of ultrasonic waves crossing the hot plume of open flames. Heat release rate disturbances are then proportional to the time rate of change of the sound travel time $\partial\Delta t/\partial t \propto \dot{Q}'$. In the case of confined flames surrounded by hot gases, fluctuations in the travel time of ultrasonic waves crossing the flame are also linked to heat release rate disturbances, but the relation must be examined in the frequency domain and is given by Eqn. 4: $\widetilde{\Delta t} = \xi(\omega)\widetilde{\dot{Q}}$.

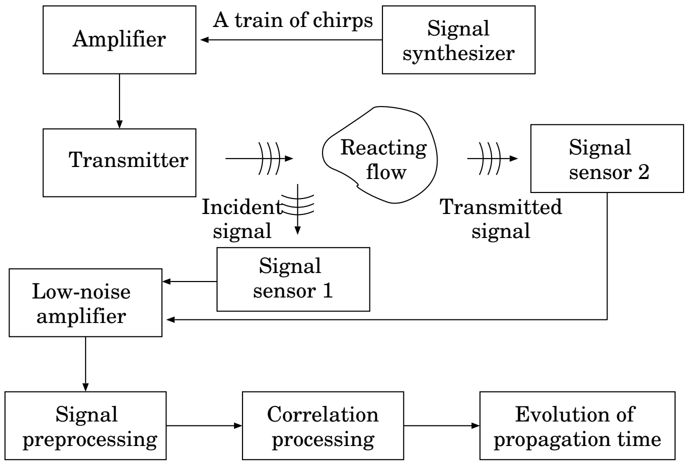

Figure 3. BLOCK DIAGRAM OF THE PULSE COMPRESSION METHOD.

3 Propagation time determination

A pulse compression technique is applied to determine the propagation time of ultrasonic waves between an emitter and a receiver [19]. Figure 3 presents the block diagram of the complete system. A train of pulses, as illustrated in Fig. 4, is synthesized by a wave generator. This signal is amplified and transmitted to space using a tweeter. The ultrasonic waves generated are measured with fixed microphones before and after their passage through the perturbed flow. These sound pressure signals are then amplified, high pass filtered and post-processed to extract the cross-correlation between the incident and transmitted sound waves. Each train of pulses is a chirp signal with a constant amplitude β but with a Linear Frequency Modulation (LFM) over a certain frequency bandwidth B and time duration τ (Fig. 4). This technique enables to obtain a narrow compressed pulse response for the cross-correlation between the incident and transmitted signals with a main peak corresponding to the sought sound travel time Δt. Provided that the repetition time t_r between two successive chirps is large enough, the time resolution of the technique improves as $1/(B\tau)$ [19–21]. Theoretically, the incident and transmitted signals can be expressed as:

$$S_i(t)=\begin{cases}\beta_i \sin\left(2\pi\left[f_i+\frac{B}{2\tau}t\right]t\right) & 0\leqslant t\leqslant\tau\\ 0 & \text{elsewhere}\end{cases}$$

$$S_t(t)=\begin{cases}\beta_t \sin\left(2\pi\left[f_i+\frac{B}{2\tau}(t-\Delta t)\right](t-\Delta t)\right) & \Delta t\leqslant t\leqslant\tau+\Delta t\\ 0 & \text{elsewhere}\end{cases}$$

The correlation between these two signals is used to obtain

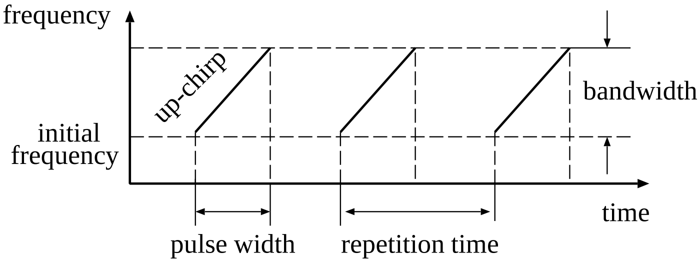

Figure 4. SCHEMATIC OF A TRAIN OF CHIRP SIGNALS.

Table 1. CHiRP PARAMETERS CHOSEN FOR THE HEAT RELEASE RATE MEASUREMENT.

	f_i [kHz]	B [kHz]	τ [ms]	t_r [ms]
without modulation	20	20	2	2.5
with modulation	20	20	0.8	1.0

a narrow compressed pulse response [22]

$$R_{\mathrm{corr}}(t) = \frac{1}{\tau}\int_{-\infty}^{+\infty} S_t^*(t')S_i(t'-t)\mathrm{d}t' \tag{10}$$

The sound propagation time Δt is determined by finding the maximum value of the envelope of the cross-correlation response. To avoid mixing different neighbor transmitted signals, the gap between two pulses $t_r - \tau$ must be larger than the fluctuations of propagation time Δt. In this study, the parameters chosen for the pulse compression technique are indicated in Tab. 1. They differ for the open flames (first line in the table) and the modulated confined flames (second line in the table) investigated in this study.

Due to the different mechanical devices in the signal generation and reception, it is not desirable to operate with square chirps characterized by large abrupt changes at the leading and trailing edges of the signal. A Hamming window is then applied to the rectangular chirp produced by the signal synthesizer to obtain a smooth transition in amplitude at the beginning and end of the chirp, but the response measured by the different sensors is still distorded. To improve results, a pre-processing applied to these raw signals is necessary. The technique is the same for the incident and transmitted signals and will only be detailed for the reference microphone M_1 in Fig. 5. The raw signal is first filtered with a high pass zero-phase shift filter to eliminate the low frequency background noise induced by the flow and the measurement chain. The filtered result is actually that shown in Fig. 5(a). A digital Butterworth filter with a cutt-off frequency f=100 Hz, an attenuation of less than 3 dB in the pass-band and at least 30 dB in the stop-band was used [23]. This filtered signal and the signal generated by the synthesizer are processed by the cross-correlation algorithm to locate the leading edge of the chirp. The resolving signal is multiplied by a rectangular box function of duration τ to eliminate the signal outside the chirp as shown in Fig. 5(b). A Hilbert transform is used to obtain the envelope of the signal, shown in Fig. 5(c). This envelope is then used to renormalize the signal presented in Fig. 5(b) and obtain a constant amplitude signal presented in Fig. 5(d).

The pre-processed signals from the reference microphone M1 and the microphone M2 are cross-correlated. The output is also processed by the Hilbert transform to keep only the envelope. The location of the peak of the main lobe returns the propagation time Δt. Figure 6 shows an example of the normalized cross-correlation. It can be noted that the level reached by the side lobes for the pre-processed response is significantly reduced compared to the result obtained without pre-processing. The resolution of the technique is indicated by the width of the main peak calculated at the level 0.5 (Fig. 6). The pre-processing clearly improves the result.

4 Experimental arrangement

Experiments are conducted on an axisymmetric burner with a 20 mm outlet nozzle diameter. Laminar premixed methane/air flames can be stabilized at the lip of the burner where the gas flow can be acoustically modulated with the loudspeaker L_2 placed at the bottom. The ultrasonic pulses crossing the burned gases are generated by the tweeter L_1 which is placed on one side of the setup. The acoustic waves are recorded by microphones M_1 and M_2 before and after the passage through the flame (B&K, type 4938). These microphones are alined so that sound waves cross on the burner symmetry axis in Fig.7. The steady and modulated flow velocities are also measured with a hot-wire placed at the exit of the burner (in absence of combustion). A photomultiplier (PM) is placed in the far-field of the flame to record the light intensity from intermediate radicals present in the flame front. For the premixed flames considered here, it is possible to estimate heat release rate perturbations $\dot{Q}'$ by examining fluctuations in the chemiluminescence intensity I of free radicals OH*, C_2* or CH* present in the reaction zone [3, 24]

$$\dot{Q}' = kI' \tag{11}$$

The coefficient k can be determined by a calibration procedure in steady operating conditions. It is a function of the experimental apparatus and the mixture composition. For premixed flames kept at a constant equivalence ratio, it is determined by changing the flowrate around the steady operating conditions.

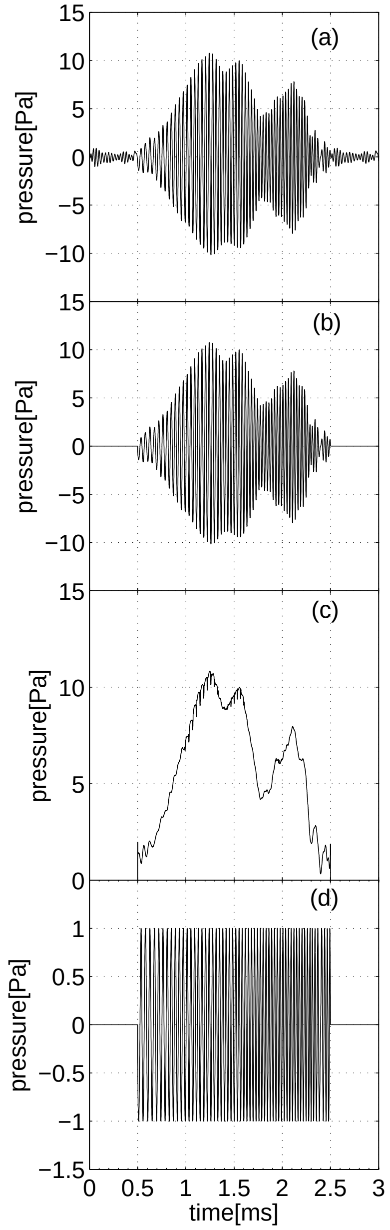

Figure 5. PRE-PROCESSING OF SIGNAL FROM M1. (a) FILTERED SIGNAL; (b) OUTPUT OF THE MULTIPLICATION BETWEEN THE FILTERED SIGNAL AND THE RECTANGULAR BOX FUNCTION; (c) ENVELOPE OF THE SIGNAL; (d) NORMALIZED SIGNAL.

A quartz tube, with an inner diameter of 50 mm and a length of 300 mm can also be placed on the top of the burner to confine the burned gases and avoid instabilities induced by buoyancy forces [25, 26]. Heat release rate fluctuations measured with the photomultiplier can be compared to that deduced from the fluctuations on the travel time of ultrasonic waves in the two configurations envisaged in this study.

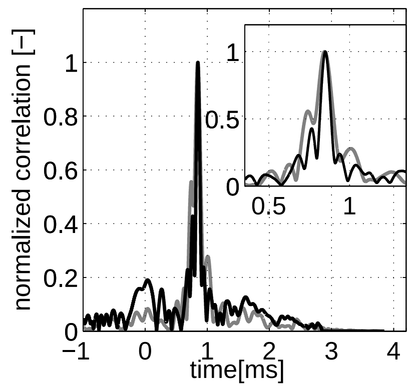

Figure 6. COMPARISON OF THE CROSS-CORRELATIONS WITH (BLACK LINE) AND WITHOUT PRE-PROCESSING (GRAY LINE).

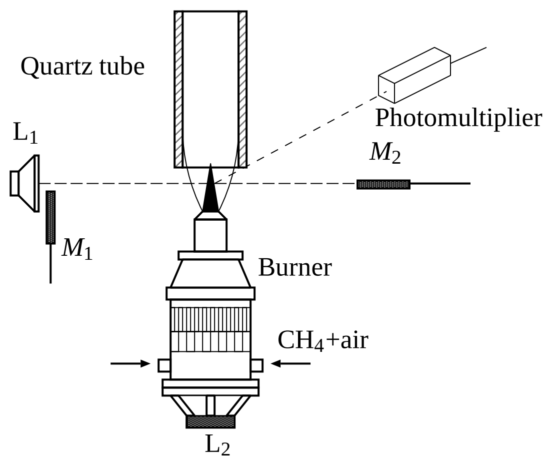

Figure 7. SCHEMATIC OF THE EXPERIMENTAL SET-UP.

5 Analysis of open flames with buoyancy effects

Flame flickering is associated to the regular oscillation of the unstable interface formed between the burned gases and ambient air, and features typical frequencies around $10-20$ Hz [11, 12]. Flickering generates small low frequency perturbations in the heat release rate. It is also known that a cylindrical tube on the top of the flame stabilizes the flow of the burned gases and the phenomenon is attenuated [25, 26]. This is illustrated in Fig. 8 where the time trace and the power spectrum of the PM are plotted for a methane/air flame (bulk velocity v_u=1.5 m s^{-1} and $\phi = 0.9$) without and with the quartz tube on the top of the flame. Fluctuations of the intensity I induced by the buoyancy forces

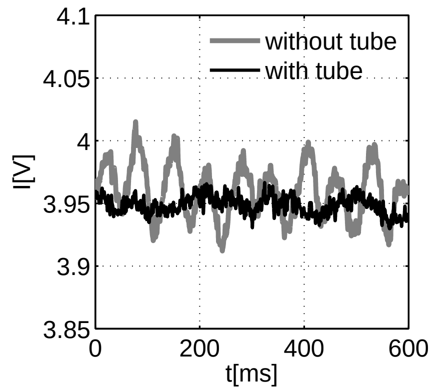

(a) Time history of PM signals.

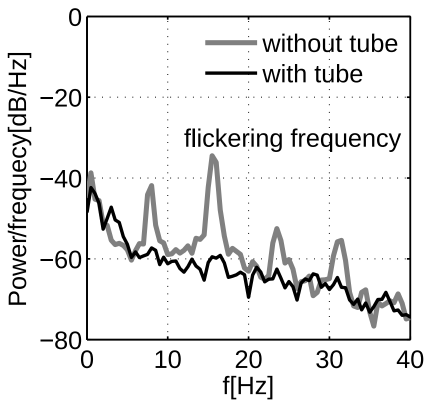

(b) Power spectrum density of PM signals.

Figure 8. TIME HISTORY AND POWER SPECTRUM DENSITY OF THE LIGHT EMISSION FROM A PREMIXED FLAME WITHOUT AND WITH THE QUARTZ TUBE: EQUIVALENCE RATIO $\phi = 0.9$, FLOW VERTICAL VELOCITY $v_u = 1.50$ m s^{-1}.

are suppressed with the tube.

Measurements of $d\Delta t/dt$ and I' were conducted for lean premixed methane/air flames with inlet flow velocities ranging from 0.84 m s^{-1} to 1.90 m s^{-1} and equivalence ratios ϕ varying from 0.85 to 1.00. Parameters fixed for the chirp generation are indicated in Tab. 1. This enables to operate with a sampling frequency equal to 400 Hz corresponding to a repetition time $t_r = 2.5$ ms. The resulting signal for $\Delta t'$ is then filtered by a low-pass zero-phase shift filter with a cut-off frequency equal to 40 Hz. The PM signal is sampled at a frequency of 8192 Hz during a period of 1.5 s and is filtered with the same low pass filter. Comparisons between the two measurements techniques are presented in Fig. 9 for three cases with different couples of equivalence ratio and flow velocity. The opposite signal $-I'$ is plotted for clarity because the proportionality coefficient Ξ between I' and $\partial\Delta t'/\partial t$ given by Eqn. 9 and Eqn. 11 is negative. The signal was also rescaled in this figure with a constant fac-

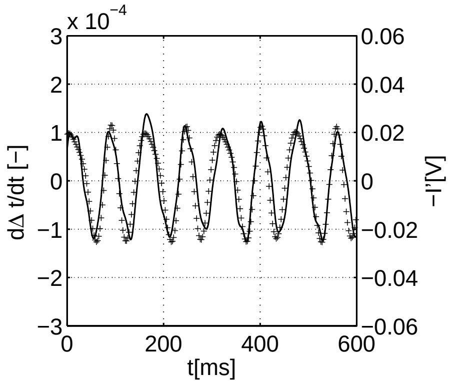

(a) $\phi = 0.85$ and $v_u = 0.84$ m s^{-1}

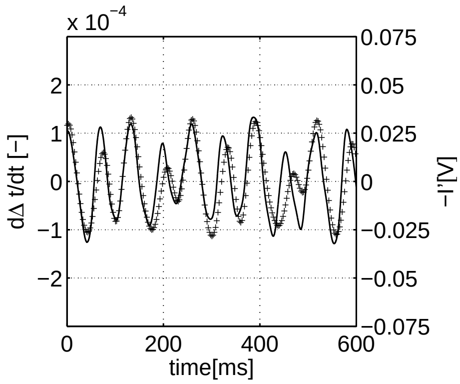

(b) $\phi = 0.85$ and $v_u = 1.68$ m s^{-1}

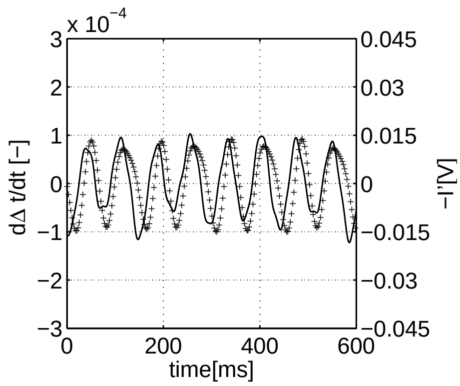

(c) $\phi = 1.00$ and $v_u = 0.84$ m s^{-1}

Figure 9. SIMULTANEOUSLY RECORDED SIGNALS $-I'$ (REPRESENTED BY THE SOLID LINE) AND $\mathrm{d}\Delta t/\mathrm{d}t$ (REPRESENTED BY THE LINE WITH MARKER $+$)

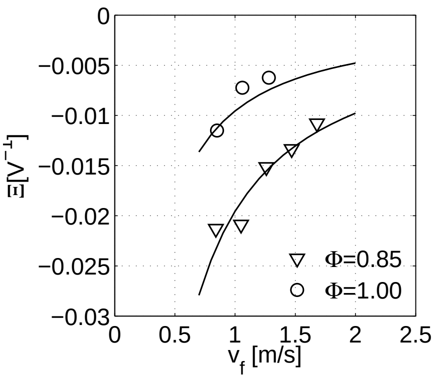

Figure 10. COMPARISON BETWEEN MEASURES AND PREDICTIONS FOR THE COEFFICIENT Ξ AT DIFFERENT EQUIVALENCE RATIOS. MARKERS $\triangledown$: $\phi = 0.85$ AND MARKERS $\circ$: $\phi = 1.0$. PREDICTIONS CORRESPOND TO THE SOLID LINES.

tor. The two signals $d\Delta t/dt$ and $-I'$ match well in phase and amplitude confirming the validity of Eqn. 9 and the sensitivity of the acoustic technique to detect small perturbations in the heat release rate. It is also possible to examine more quantitatively the validity of Eqn. 9 by plotting predictions for the coefficient Ξ in Fig. 10 which are compared to measurements for two different equivalence ratios $\phi = 0.85$ and $\phi = 1.00$ as a function of the nozzle outlet flow velocity. The numerical values used to estimate Ξ are listed in Tab. 2. The distribution of experimental results still match well with the predictions.

Table 2. NUMERICAL VALUES USED FOR COMPUTATION OF THE COEFFICIENT Ξ

ϕ	S_L [m s^{-1}]	c_u [m s^{-1}]	c_b [m s^{-1}]	k [kW V^{-1}]	α
0.85	0.31	343	797	3.11	0.1
1.00	0.38	343	834	5.79	0.1

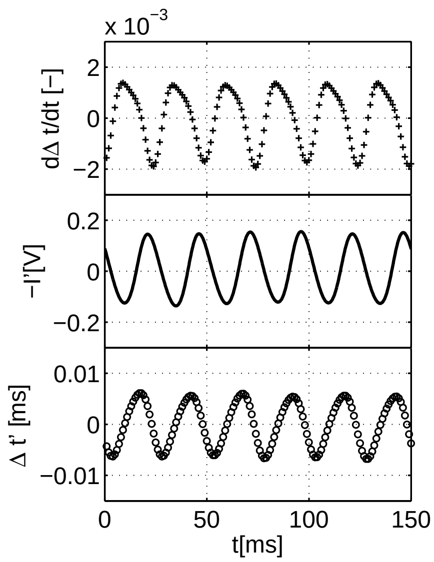

(a) $f_m = 40$ Hz, $\phi = 1$, $\bar{v}_u = 1.5$ m s^{-1} and $v'_u = 0.13$ m s^{-1}

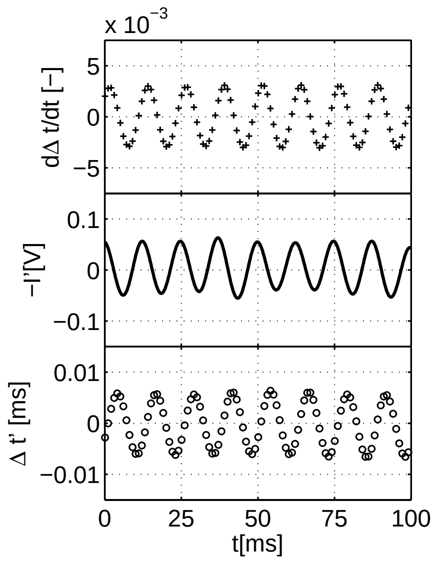

(b) $f_m = 80$ Hz, $\phi = 1$, $\bar{v}_u = 1.5$ m s^{-1} and $v'_u = 0.13$ m s^{-1}

Figure 11. COMPARISON BETWEEN FLUCTUATIONS OF THE TRAVEL TIME WITH THE CHEMILUMINESCENCE SIGNAL AT TWO DIFFERENT MODULATION FREQUENCIES. PLOTS ARE $\mathrm{d}\Delta t/\mathrm{d}t$ (TOP GRAPH), $-I'$ (MIDDLE GRAPH) AND $\Delta t'$ (BOTTOM GRAPH).

6 Analysis of confined flames submitted to flow modulation

The case of lean premixed methane/air confined flames submitted to flow disturbances is now examined. The quartz tube is placed on the top of the setup to hind buoyancy effects and the loudspeaker is used to produce harmonic flow modulations. The modulation frequency f_m varies from 20 Hz to 100 Hz and the velocity perturbation amplitude v'_u covers 0.07 to 0.40 m s^{-1}.

The chirp signal parameters are now given by the second line in Tab. 1. This enables to use a higher sampling frequency of 1 kHz corresponding to a shirp repetition time $t_r = 1$ ms. This is necessary to obtain a good resolution in the determination of the heat release rate with the acoustic technique at the largest modulation frequency envisaged here $f = 100$ Hz. The processing of the measured sound travel time and the PM output is the same as in the previous section but with a larger cut-off frequency equal to 200 Hz. The axial velocity signal at the burner outlet is determined with a hot-wire in absence of combustion and writes

$$v_u = \bar{v}_u + v'_u \sin(2\pi f_m t) \tag{12}$$

Comparisons for a stoechiometric mixture between the records of $d\Delta t/dt$, I' and $\Delta t'$ are shown in Fig. 11 for two modulation frequencies $f_m = 40$ and 80 Hz at a fixed input level $v'_u = 0.13$ m s^{-1}. The responses delivered by the PM and the acoustic technique correspond nearly to harmonic signals with the same frequency as the velocity forcing signal. This is confirmed in Fig. 12 where the power spectra of the fluctuations in the sound travel time $\Delta t'$ and in the chemiluminescence intensity I' are plotted. The response of these signals clearly follows the modulation for the two forcing frequencies. It is however visible in Fig. 11 that the time rate of change of the sound travel time $d\Delta t/dt$ is not in phase with the fluctuations observed in the chemiluminescence signal $-I'$ as it was the case for the flame submitted to buoyancy forces investigated in the previous section.

Equation 9 does not apply to confined flames. It is preferable to directly compare fluctuations in the sound travel time $\Delta t'$ to disturbances in the chemiluminescence intensity signal I' as suggested in Eqn. 4. It is in particular found that the phase shift between these two signals is higher for a modulation frequency $f_m = 80$ Hz than at $f_m = 40$ Hz. This is consistent with the conjecture made in Section 2, that the phase shift between fluctuations in the sound travel time and the heat release rate increases with increasing the forcing frequency. Further validations with more detailed comparisons are necessary to determine the exact link between these two signals. This will be the object of future work. It can nonetheless be concluded that it is possible to detect heat release rate fluctuations with the acoustic methodology proposed in this study for confined flames submitted to flow modulations.

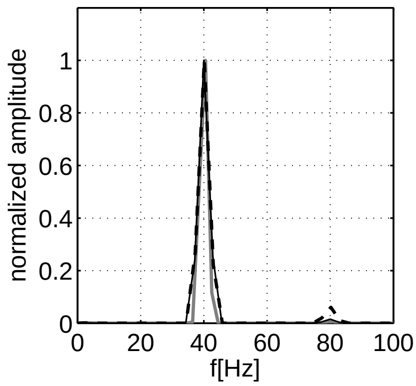

(a) $f_m = 40$ Hz, $\phi = 1$, $\bar{v}_u = 1.5$ m s^{-1} and $v'_u = 0.13$ m s^{-1}

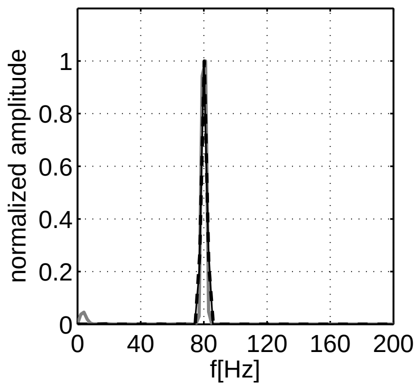

(b) $f_m = 80$ Hz, $\phi = 1$, $\bar{v}_u = 1.5$ m s^{-1} and $v'_u = 0.13$ m s^{-1}

Figure 12. NORMALIZED POWER SPECTRA OF THE SIGNALS $d\Delta t/dt$ (dotted lines), I' (GRAY SOLID LINE) AND $\Delta t'$ (BLACK SOLID LINE) FOR TWO MODULATIONS FREQUENCIES.

7 Conclusion

It has been shown that it is possible to estimate heat release rate perturbations based on the knowledge of fluctuations in the sound propagation time of ultrasonic waves crossing a flame. This has led to the development of an acoustic methodology to determine small changes in the sound propagation time of high frequency acoustic waves using a pulse compression technique. First validations were conducted in two generic configurations with a tweeter to generate the sound waves and microphones to record the incident and transmitted signals. It was possible to detect small heat release rate disturbances driven by buoyancy forces in open flames indicating that the technique is very sensitive. The temporal resolution of the technique depends on the compression factor $B\tau$ where B is the chirp bandwidth and τ the chirp duration. It is thus necessary to reduce the chirp duration τ and go to higher frequencies to obtain time resolved results of heat release rate perturbations at high frequencies. This will be the object of future developments by changing the material to ultrasonic transmitters and receivers. Examination of the theoretical link between fluctuations in the sound travel time and heat release rate is also in progress. Detailed validations in more complex flow configurations are envisaged as well. The objective is to develop an alternative technique to optical diagnostics when access is limited.

8 Acknowledgement

Jingxuan Li is supported by a doctoral fellowship from China Scholarship Council, Project 111, Grant No. B08009. The authors wish to thank D. Durox for helpful discussion about buoyancy effects.

REFERENCES

[1] Candel, S., 2002. "Combustion dynamics and control: Progress and challenges". *Proceedings of the Combustion Institute,* ***29***(1), pp. 1 – 28.

[2] Hurle, I. R., Price, R. B., Sugden, T. M., and Thomas, A., 1968. "Sound Emission from Open Turbulent Premixed Flames". *Royal Society of London Proceedings Series A,* ***303***, Mar., pp. 409–427.

[3] Price, R., Hurle, I., and Sugden, T., 1969. "Optical studies of the generation of noise in turbulent flames". *Symposium (International) on Combustion,* ***12***(1), pp. 1093 – 1102.

[4] Higgins, B., McQuay, M. Q., Lacas, F., and Candel, S., 2001. "An experimental study on the effect of pressure and strain rate on ch chemiluminescence of premixed fuel-lean methane/air flames". *Fuel,* ***80***(11), pp. 1583 – 1591.

[5] Hardalupas, Y., and Orain, M., 2004. "Local measurements of the time-dependent heat release rate and equivalence ratio using chemiluminescent emission from a flame". *Combustion and Flame,* ***139***(3), pp. 188 – 207.

[6] Lauer, M., and Sattelmayer, T., 2010. "On the adequacy of chemiluminescence as a measure for heat release in turbulent flames with mixture gradients". *Journal of Engineering for Gas Turbines and Power,* ***132***(061502), pp. 1–8.

[7] Schuller, T., Durox, D., and Candel, S., 2002. "Dynamics of and noise radiated by a perturbed impinging premixed jet flame". *Combustion and Flame,* ***128***(1-2), pp. 88 – 110.

[8] Fayoux, A., Zähringer, K., Gicquel, O., and Rolon, J., 2005. "Experimental and numerical determination of heat release in counterflow premixed laminar flames". *Proceedings of the Combustion Institute,* ***30***(1), pp. 251 – 257.

[9] Ayoola, B., Balachandran, R., Frank, J., Mastorakos, E., and Kaminski, C., 2006. "Spatially resolved heat release rate measurements in turbulent premixed flames". *Combustion and Flame,* ***144***(1-2), pp. 1 – 16.

[10] Lieuwen, T., 2001. "Theory of high frequency acoustic wave scattering by turbulent flames". *Combustion and Flame,* ***126***(1-2), pp. 1489 – 1505.

[11] D. Durox, T., and E.Villermaux, 1997. "The effect of buoyancy on flickering in diffusion flames". *Combustion Science and Technology,* ***124***, pp. 277–294.

[12] Kostiuk, L., and Cheng, R., 1994. "Imaging of premixed flames in microgravity". *Experiments in Fluids,* ***18***, pp. 59–68.

[13] Ducruix, S., Thierry, S., Durox, D., and Candel, S., 2003. "Combustion dynamics and instabilities: Elementary coupling and driving mechanisms". *Journal of propulsion and power,* ***19***(5), pp. 722–734.

[14] Fleifil, M., Annaswamy, A. M., Ghoneim, Z. A., and Ghoniem, A. F., 1996. "Response of a laminar premixed flame to flow oscillations: A kinematic model and thermoacoustic instability results". *Combustion and Flame,* ***106***(4), pp. 487 – 510.

[15] Dowling, A. P., 1999. "A kinematic model of a ducted flame". *Journal of Fluid Mechanics,* ***394***, pp. 51–72.

[16] Schuller, T., Durox, D., and Candel, S., 2003. "A unified model for the prediction of laminar flame transfer functions: comparisons between conical and V-flame dynamics-flame dynamics". *Combustion and Flame,* ***134***(1-2), pp. 21 – 34.

[17] Cho, J. H., and Lieuwen, T., 2005. "Laminar premixed flame response to equivalence ratio oscillations". *Combustion and Flame,* ***140***(1-2), pp. 116 – 129.

[18] Palies, P., Schuller, T., Durox, D., and Candel, S., 2011. "Modeling of premixed swirling flames transfer functions". *Proceedings of the Combustion Institute,* ***33***(2), pp. 2967 – 2974.

[19] Merrill, S., 2008. *Radar Handbook, 3rd Edition*. McGraw-Hill.

[20] Klauder, J., Price, A. C., Darlington, S., and Albersheim, W. J., 1960. "The theory and design of chirp radars". *The bell system technical journal,* ***39***(4), July, pp. 745–808.

[21] Cook, C. E., and Bernfield, M., 1967. *Radar Signals: An Introduction to Theory and Application*. Artech House Publishers.

[22] Mahafza, B. R., and Elsherbeni, A. Z., 2004. *Matlab Simulations for Radar Systems Design*. Chapman and Hall.

[23] Oppenheim, A. V., and Schafer, R., 1975. *Digital signal processing*. Prentice-Hall.

[24] Ducruix, S., Durox, D., and Candel, S., 2000. "Theoretical and experimental determinations of the transfer function of a laminar premixed flame". *Proceedings of the Combustion Institute,* ***28***(1), pp. 765 – 773.

[25] Kizirnis, S. W., Brecha, R. J., Ganguly, B. N., Goss, L. P., , and Gupta, R., 1984. "Hydroxyl (OH) distributions and temperature profiles in a premixed propane flame obtained by laser deflection techniques". *Applied Optics,* ***23***, pp. 3873–3880.

[26] Linteris, G., and Rafferty, I., 2008. "Flame size, heat release, and smoke points in materials flammability". *Fire Safety Journal,* ***43***(6), pp. 442 – 450.

